Title
IMPEDANCE OF LITHIUM ELECTRODES IN A PROPYLENE CARBONATE ELECTROLYTE

Authors
Thevenin, J.G.
Muller, R.H.

Publication Date
1986-02-01

Lawrence Berkeley Laboratory
UNIVERSITY OF CALIFORNIA

Materials & Molecular Research Division

Submitted to Journal of the
Electrochemical Society

IMPEDANCE OF LITHIUM ELECTRODES IN A PROPYLENE CARBONATE ELECTROLYTE

J.G. Thevenin and R.H. Muller

February 1986

Prepared for the U.S. Department of Energy under Contract DE-AC03-76SF00098

DISCLAIMER

LBL-21192

IMPEDANCE OF LITHIUM ELECTRODES IN A PROPYLENE CARBONATE ELECTROLYTE

J.G. Thevenin and R.H. Muller

Lawrence Berkeley Laboratory

University of California

Berkeley, CA 94720

February 1986

ABSTRACT

Different models of compact, porous, composite, and stratified surface layers have been investigated for the interpretation of impedance measurements of lithium electrodes in organic electrolytes. The surface layers are assumed to consist of organic and inorganic compounds with the properties of solid and polymer electrolytes. Comparison of predicted impedance spectra with those measured for surface layers formed in a molar solution of lithium perchlorate in propylene carbonate shows that two interphase models can be used to derive from the impedance measurements the thickness of surface layers in agreement with previous ellipsometric measurements. In a compact-stratified layer (CSL) model, the surface layer is assumed to consist of two sublayers of solid electrolyte with different conductivities; in a solid-polymer interphase (SPI) model, the surface layer is assumed to consist of a mixture of solid and polymer electrolytes.

INTRODUCTION

The thermodynamic instability of lithium in contact with most nonaqueous battery electrolytes leads to the formation of layers on electrode surfaces that can result in an unexpected electrochemical behavior of the lithium electrode.[1,2]

Propylene carbonate-based electrolytes have been studied extensively. The morphological characteristics of the surface layer have been studied by scanning electron microscopy,[3,4] transmission electron microscopy,[5] Auger spectroscopy,[6] photoelectron spectroscopy,[7] ellipsometry,[8] and x-ray diffraction.[9] The kinetic properties of the surface layer have been studied by means of stationary polarization,[10,11] cyclic voltammetry,[12] potentiostatic and galvanostatic pulse techniques,[13] and electrode-impedance spectroscopy.[14] Two principal results of these studies are: (1) The surface layer, which contains the products of reactions between lithium and the solvent, the salt, and their impurities, is composed of various organic and inorganic compounds. (2) The surface layer can be an ionic conductor and an electronic insulator, and it acts as an interphase between the lithium electrode and the organic electrolyte. The properties of such a surface layer can be those of a solid electrolyte[13] and/or a porous insulating membrane[14] depending on the purification procedure used for the organic electrolyte. Even in the well-known propylene carbonate-based electrolytes,[15-24] the composition

and structure of the surface layer is not well understood. The presence of successive sublayers made of different organic and inorganic compounds has been assumed.[24] Use of the models presented in the literature[13,14] can lead to misinterpretations of such systems.

In the present work, electrode-impedance spectroscopy has been used to study the electrochemical properties of surface layers on lithium electrodes. Different models of compact, porous composite, and stratified interphases with the properties of solid and polymer electrolytes have been investigated to derive the thickness of surface layers from the impedance measurements.

THEORETICAL

Impedance Behavior for Different Interphase Models

The metal/surface-layer/solution system involved in the impedance behavior of the lithium electrode covered by a surface layer formed in an organic electrolyte can be studied under some simplifying assumptions. The surface layer is assumed to be an ionic conductor and an electronic insulator. The impedance of this completely nonblocking system[25] is represented by the equivalent circuit of the surface layer independent of the solution resistance. Many different equivalent circuits can be defined for various compositions and structures, but only a few simple circuits can be used in practice for the analysis of the impedance measurements. The interphase models have been developed for compositions which result in surface layers with properties of a solid

or a polymer electrolyte. These surface layers may have a compact, porous, composite, or a stratified structure. The following interphase models have been studied by their equivalent circuits, and their impedance behaviors have been analyzed.

1. Compact Layers

Two main compositions of the surface layer can be defined according to morphological studies presented in the literature. The first composition corresponds to compact inorganic compounds with the properties of a solid electrolyte[20,25] (the SEI model). The second composition corresponds to a compact mixture of organic and inorganic compounds with the properties of a polymer electrolyte[27,28] (the PEI model). These two models are analyzed in greater detail below.

1a. The Solid-Electrolyte Interphase (SEI) Model

The equivalent circuit and impedance diagram of the SEI layer are shown in Fig. 1. This circuit consists of the bulk resistance R_b and the geometric capacitance C_g both of which are related to the conduction process in the solid electrolyte. The corresponding impedance diagram in the complex plane consists of a semicircle due to the R_b/C_g coupling over the whole frequency range. By analyzing this diagram one can determine the thickness of the surface layer for a known permittivity or conductivity of the solid electrolyte. (see Appendix I).

1b. The Polymer-Electrolyte Interphase (PEI) Model

The equivalent circuit and impedance diagram related to the PEI

layer are given in Fig. 2. The equivalent circuit is determined by three types of impedances: (1) The conduction impedance defined by the bulk resistance R_b and the geometric capacitance C_g; (2) The charge transfer impedance represented by the charge transfer resistance R_{ct} and the double-layer capacitance C_{dl}; (3) The diffusion impedance Z_d corresponding to a finite thickness of the diffusion layer.[29] The impedance diagram in the complex plane exhibits three features: (1) A semicircle in the high-frequency range, due to the R_b/C_g coupling; (2) A semicircle in the intermediate-frequency range, due to the R_{ct}/C_{dl} coupling; and (3) A characteristic loop in the low-frequency range due to Z_d. By analyzing this diagram, especially the conduction loop, one can determine the thickness of the surface layer provided that either the conductivity or the permittivity is known. (see Appendix II).

2. Porous Layers

The porosity of the surface layer results from its formation by the decomposition of the organic solvent and dissolved electrolyte in presence of lithium. The impedance behavior of the surface layer can be represented by a transmission-line model for which the finite thickness of the porous system is recognized.[30] In general, the total impedance depends on the relative importance of the impedances of the solid and liquid phases (the PLI model). A limiting case is obtained when the surface layer is formed by a porous insulating membrane[31,32] (the PIM model). The two models are analyzed in greater detail below.

2a. The Porous-Layer Interphase (PLI) Model

As the usual simplifying assumptions for a transmission-line model,[30] the surface layer is assumed to have straight parallel and cylindrical pores of uniform diameter and constant composition, as shown in Fig. 3. Four distinct impedances are involved in the total impedance: (1) The liquid-phase impedance per unit pore length Z_l, related to the properties of the organic electrolyte filling the pores. (2) The solid-phase impedance per unit pore length Z_s, determined by the properties of the surface layer. (3) The impedance occurring on the pore base Z_b independent of the pore length representing the impedance of the electrode/liquid-phase interface. (4) The admittance occurring on the pore wall per unit pore length $1/Z_p$, representing the admittance of the solid-phase/liquid-phase interface. All the information can be derived by fitting the curve of the measured impedance diagram to the general equation of the total impedance. In practice, however, because of the large number of parameters involved in the equation, the curve fitting technique is not accurate enough or unique for the determination of the thickness of the surface layer even when the different impedances Z_l, Z_s, Z_b and Z_p for a planar system are known.

2b. The Porous-Insulating Membrane (PIM) Model

A limiting case of a porous system is obtained when the surface layer is assumed to be formed by an insulating material such as a polymeric membrane.[31,32] Thus, the impedances Z_s and Z_p are several order of magnitude larger than the impedances Z_l and Z_b. Under these

conditions, the equivalent circuit and impedance diagram related to the PIM model can be defined as shown in Fig. 4. The equivalent circuit of the active surface area (1-Θ) is represented by the Randles circuit, while the equivalent circuit of the passive surface area (Θ) is represented by R_m and C_m determined by the resistive and dielectric properties of the membrane. The corresponding impedance diagram in the complex plane consists of two parts: (1) a semicircle in the high-frequency range, resulting from the coupling R_{ct}/C_{dl} related to the charge-transfer process on the active surface, and (2) a characteristic loop in the low-frequency range resulting from the impedance Z_d due to the diffusion of the species through the pores. By analyzing this diagram one can determine the thickness of the surface layer provided that the double-layer capacitance on the free metal surface is known.

The present terminology of Porous-Insulating Membrane (PIM) Model for this kind of surface layer[32] replaces the earlier used term of Polymer-Electrolyte Interphase (PEI) Model because it is not referring to a surface layer with the general properties of a compact polymer electrolyte.

3. Composite and Stratified Layers

The presence of organic and inorganic compounds in the surface layer suggests a complex composition, which may be represented by a composite material. A limiting case is to consider that the surface layer has the average properties of both solid and polymer electrolytes which are

mixed to form a compact solid-polymer layer (the SPI Model). Other models are based on the assumption that the surface layer consists of two different compact or porous sublayers. A stratified structure can be due to the presence of a solid electrolyte on the electrode surface and a solid or a polymer electrolyte facing the organic electrolyte (the CSL Model). Another stratified structure can be defined by a compact solid electrolyte on the electrode surface and a porous insulating membrane facing the organic electrolyte (the PSL Model). All three of these models are analyzed in greater detail below.

3a. The Solid-Polymer Interphase (SPI) Model

In this model, the surface layer is assumed to consist of solid compounds dispersed in a polymeric matrix. As shown in Fig. 5, the equivalent circuit of the lithium covered by such a solid-polymer interphase can be similar to that of the PEI Model. In the SPI case, the different time constants of the conduction, charge transfer, and diffusion processes may not be well separated. The three loops mix to form a distorted loop, which can only suggest the existence of the different processes. Nevertheless, the impedance data can be analyzed with sufficient accuracy by using the Cole-Cole and Bode plots for depressed and overlapped semicircles (see Appendix II). Assuming that the conduction process can be separated from the other processes by a geometric fitting between the experimental and computer-generated impedance diagrams, the main parameters of the surface layer can be evaluated, provided that either the permittivity or the conductivity is

known.

3b. The Compact-Stratified Layer (CSL) Model

In this model, the surface layer is assumed to be made of two sublayers as shown in Fig. 6. The first sublayer is a solid electrolyte on the electrode surface, and the second sublayer is either a solid or a polymer electrolyte in contact with the solution. For this model, the equivalent circuit can be represented by a unique R_iC_i circuit by taking into account the integral values of the bulk resistance and geometrical capacitance of the surface layer (see Appendix I). The corresponding impedance diagram in the complex plane is a semicircle over the whole frequency range. By analyzing this diagram one can determine the total thickness of the surface layer as well as the thickness of each sublayer provided that either the two permittivities or the two conductivities are known.

3c. The Porous-Stratified Layer (PSL) Model

In this model, the surface layer is assumed to be made up of two sublayers, as shown in Fig. 7. The first sublayer is a compact solid electrolyte on the electrode surface, and the second sublayer is a porous insulating membrane in contact with the solution. For this model the equivalent circuit can be represented by the circuit of the SEI layer placed in series with the circuit of the PIM layer. The corresponding impedance diagram in the complex plane consists of three loops but only when the time constants of the processes are well separated. The first loop in the high-frequency range can be attributed to the conduction process. The second loop in the

intermediate-frequency range is due to the charge-transfer process. The third loop in the low-frequency range is related to the diffusion of the species through the pores of the membrane. By analyzing this impedance diagram one can determine the thickness of the compact solid electrolyte and of the porous insulating membrane, using the SEI and PIM models previously discussed.

EXPERIMENTAL

1. Organic Electrolyte

The electrolyte studied was the molar solution of lithium perchlorate in propylene carbonate with a residual water content of a few ppm. Propylene carbonate (Burdick and Jackson Lab.) was dehydrated on molecular sieves of 3-A mesh for about 2 weeks. Lithium perchlorate (Smith Chem. Co.) was dessicated at 240^{o}C for one day under a vacuum created by a mechanical pump. The molar solution was prepared in an inert atmosphere with the dehydrated solvent and the dessicated solute, and treated by lithium amalgam for 7 hours (50 cm^3 of solution for 1 cm^3 of lithium amalgam). The gray Li(Hg) powder was formed by immersing 1.5 wt% or more of lithium in mercury.

2. Electrolytic Cell

The electrolytic cell, made of polypropylene, had two openings for inserting the working and counter electrodes, and a compartment for extruding the lithium reference electrode. The working electrode was

the cross section of a lithium cylinder of 0.2 cm diameter extruded from a polypropylene holder. The counterelectrode was a lithium disc of 2 cm diameter and 0.1 cm thickness, which was inserted into a polypropylene holder. The reference electrode was the cross section of a lithium cylinder of 0.2 cm diameter. The reference and working lithium electrodes were cut with a blade under inert atmosphere just before immersion into the electrolyte. The reference electrode was cut frequently during the experiment to avoid any artefacts due to its impedance.

3. Impedance Measurements

The electrode impedance was determined using the lock-in amplifier technique in the high-frequency range (5×10^4 to 5 Hz) and the Lissajous-figure technique in the low-frequency range (5 to 5×10^{-3} Hz). The system was used in the galvanostatic mode near the open-circuit potential of the lithium electrode. The alternating-current density was about 0.05 mA/cm^2, which provided a linear response, as required for valid electrode-impedance measurements. The equipment included an oscillator (Hewlett Packard Model 3310A), which drove a potentiostat-galvanostat (Princeton Applied Research Model 173). The oscillating current and voltage were measured by a differential preamplifier (Princeton Applied Research Model 113). The in-phase and out-of-phase components of the current and voltage were determined with two lock-in amplifiers (Princeton Applied Research Model 5101). Current versus voltage was displayed on a storage

oscilloscope (Tektronix Model 5111).

RESULTS AND DISCUSSION

1. Layer Composition

Many different compounds can result from the reaction between lithium and the solution of lithium perchlorate in propylene carbonate. The chemical decomposition of propylene carbonate in the presence of lithium has been reported to result in the formation of propylene and Li_2CO_3.[17,18] The occurrence of this reaction is supported by the evolution of gas and the formation of a solid precipitate during the immersion of lithium amalgam in the organic solvent. But a polymerization of propylene carbonate can also be observed at times. For example, the immersion of a small amount (0.1 cm^3) of lithium amalgam in a large volume (50 cm^3) of solution can result in the conversion of the entire liquid volume to a colorless polymer that contains bubbles after one day. Thus it is possible that polypropylene oxide P(PO) and carbon dioxide is formed. Since lithium perchlorate can form a polymer electrolyte with polypropylene oxide,[27,28] one can expect the formation of $P(PO)_x$ $LiClO_4$, where x is the lithium/oxygen ratio. Thus the surface layer resulting from a dry solution can be a mixture of a solid electrolyte Li_2CO_3 and a polymer electrolyte $P(PO)_x$ $LiClO_4$. Since a reactive impurity in propylene carbonate is water, the formation of Li_2O and LiOH is also expected. Li_2O has been assumed to be on the lithium surface, while LiOH may be located between the oxide

and the wet solution.[33] Other compounds such as LiCl can result from the decomposition of $LiClO_4$ in the presence of lithium.[5,7] All these decomposition reactions may be the cause of the formation of complex solids and polymers on the surface of the lithium electrode.

2. Impedance Data

The study of the electrochemical properties of surface layers was carried out for two weeks at the open-circuit potential in the molar solution of lithium perchlorate in propylene carbonate treated with lithium amalgam. The impedance diagrams, plotted in the complex plane, for different storage times are detailed in Figs. 8 through 11.

During the first day of growth of the surface layer, as shown in Fig. 8, the impedance diagram in the complex plane exhibits two features: (1) in the high-frequency range, a semicircle, which can be related to a charge transfer process, and (2) in the low-frequency range, a straight line which is characteristic of a diffusion process. The increase of the semicircle with the decrease of the straight line as a function of the storage time indicates a fast change of the processes involved in the formation of the surface layer. This change is certainly related to an important modification in composition and structure of the surface layer.

During the next days, as shown in Figs. 9 through 11, the impedance diagrams exhibit only one depressed loop over the whole frequency range. This loop can be defined by the apparent resistance R_a and capacitance C_a, which are functions of the storage time, as

shown in Fig. 12. Because the product $R_a C_a$, which is the apparent time constant of the system, has an increasing value as a function of the storage time, it seems too simple to attribute the loop to a simple conduction process in a solid electrolyte according to the Solid-Electrolyte Interphase (SEI) model. Nevertheless, it is interesting to use this model for a rough estimation of the thickness of the surface layer during the storage. Taking into account the apparent capacitance C_a, as shown in Fig. 13, the layer thickness Y increases as an exponential function of the storage time from 15 or 30 A to 25 or 50 A for a relative permittivity $_r$ equal to 5 or 10, corresponding to a solid electrolyte such as Li_2CO_3 or Li_2O, respectively.[13,20] As shown in Fig. 14, by taking into account the apparent resistance R_a, the layer thickness increases as an other exponential function of the storage time from 5 or 10 A to 100 or 200 A for a conductivity equal to 1 or 2 x 10^{-9} $^{-1}cm^{-1}$. These values derived from impedance measurements are much lower than the values (up to 1500 A) determined by ellipsometric measurements performed by Schwager, Geronov and Muller,[6,8] using similar experimental conditions. According to these authors, the discrepancy between the optical and electrochemical thicknesses can be attributed to the sensitivity of the respective methods in detecting the different parts of the surface layer.

3. Interpretation

The surface layer can be considered to be made of two sublayers with different permittivities and conductivities, according to the Compact-Stratified Layer (CSL) Model. The use of this model (see Appendix I) leads to a new evaluation of the total thickness of the surface layer, as shown in Fig. A1. In this study, it is assumed that the first sublayer has the properties of a solid electrolyte Li_2CO_3 ($\varepsilon_1 = 5\varepsilon_o$, $\sigma_1 = 1 \times 10^{-9}\ \Omega^{-1}cm^{-1}$), and the second sublayer has the properties of a polymer electrolyte $P(PO)_xLiClO_4$ ($\varepsilon_2 = 50\varepsilon_o$, $\sigma_2 = 50 \times 10^{-9}\ \Omega^{-1}cm^{-1}$). As shown in Fig. 13, for a ratio $\varepsilon_1/\varepsilon_2$ equal to 10, the total thickness L ranges only from 75 to 125 Å. Thus, this assumption concerning the variation of the permittivity appears not valid to obtain an agreement between the optical and electric measurements. But the other possible assumption concerning the variation of the conductivity seems to be more appropriate. As shown in Fig. 14, for a ratio σ_1/σ_2 equal to 50, the total thickness L ranges from 100 to 1500 Å during two weeks of storage. For this example, the thickness d of the first sublayer ranges from 10 to 100 Å, while the thickness (L-d) of the second sublayer ranges from 90 to 1400 Å. These values of the thickness of the surface layer deduced from the impedance data, according to the CSL model for the case of a variation of the conductivity, appears in good agreement with those deduced from the ellipsometric data.[8]

The surface layer can also be considered as a solid-polymer electrolyte to be made of Li_2CO_3 and $P(PO)_xLiClO_4$, the properties of which are analyzed in the Solid-Polymer Interphase (SPI) Model. For this model, the depressed semicircle in the complex plane is assumed to be made of three semicircles due to the conduction, charge transfer, and diffusion processes with similar time constants. The use of this model (see Appendix II) needs the identification of the conduction process for the determination of the parameters of its equivalent circuit. The analysis of the Figs. 9 through 11 demonstrates that the impedance diagrams are progressively distorted by the occurrence of more than one time constant after the 7th day of storage. Considering successive resistance/capacitance circuits with a same depression parameter, an approximate geometrical fitting between the experimental and theoretical Cole-Cole and Bode plots can be obtained for example, for three time constants after 11 days of storage, as shown in Fig. A2. The study of the apparent resistance R_a (capacitance C_a) in order to define its different components R_1, R_2 and R_3 (C_1, C_2 and C_3) is shown in Fig. 15 between the 7th and 15th day of storage. Assuming that the first loop in the high-frequency range (coupling R_1/C_1) is related to the conduction process in the surface layer, the thickness of the surface layer can be determined for either a given permittivity or conductivity. As shown in Fig. 16, the thickness of the surface layer increases exponentially from 500 to 1000 Å for a permittivity equal to 50, and from 175 to 1125 Å for a conductivity equal to $50 \times 10^{-9} \Omega^{-1} cm^{-1}$. These last values of the thickness of the surface layer appear

also in agreement with those deduced from ellipsometric measurements.[8]

CONCLUSION

The study of the impedance behavior of the metal/surface-layer/solution system has shown that several interphase models of the surface layer can be defined if one knows its composition and structure. But the determination of the thickness of the surface layer is only possible when the conduction process is well separated from the other processes involved in the system, and when the permittivity or the conductivty of the surface layer is known by another method. For the case of good ionic conductors, different interphase models have been discussed for surface layers having the general properties of either a solid or a polymer electrolyte. The equivalent circuit and the corresponding impedance diagram have been analyzed for compact, porous, composite, and stratified surface layers.

The study of the impedance behavior of the lithium electrode in a lithium perchlorate/propylene carbonate solution has shown that the surface layer can be considered as either a compact-stratified layer (CSL) or a solid-polymer interphase (SPL). Compounds such as Li_2O, Li_2CO_3, and $P(PO)_xLiClO_4$ have been considered according to the main decomposition products of the organic electrolyte studied. The fact that the thicknesses of the surface layer deduced from the impedance measurements are in good agreement with those deduced from ellipsometric measurements suggests that the CSL and SPI models may be

useful for understanding the main properties of the surface layers formed on the lithium electrode in organic electrolytes.

ACKNOWLEDGMENTS

This work was supported by the Assistant Secretary for Conservation and Renewable Energy, Office of Advanced Conservation Technologies, Electrochemical Research Division of the U.S. Department of Energy under Contract No. DE-AC03-76SF00098.

FIGURE CAPTIONS

Fig. 1. The Solid-Electrolyte Interphase (SEI) Model. Schematic view, equivalent circuit, and corresponding impedance diagram.

Fig. 2. The Polymer-Electrolyte Interphase (PEI) Model. Schematic view, equivalent circuit, and corresponding impedance diagram.

Fig. 3. The Porous-Layer Interphase (PLI) Model. Schematic view equivalent circuit, and corresponding impedance diagram.

Fig. 4. The Porous-Insulating Membrane (PIM) Model. Schematic view, equivalent circuit, and corresponding impedance diagram.

Fig. 5. The Solid-Polymer Interphase (SPI) Model. Schematic view, equivalent circuit, and corresponding impedance diagram.

Fig. 6. The Compact-Stratified Layer (CSL) Model. Schematic view, equivalent circuit, and corresponding impedance diagram.

Fig. 7. The Porous-Stratified Layer (PSL) Model. Schematic view, equivalent circuit, and corresponding impedance diagram.

Fig. 8. Impedance diagram in the complex plane obtained with a lithium electrode immersed in the molar solution of lithium perchlorate in propylene carbonate. a) after 30 min., b) after 2 hours, c) after 6 hours.

Fig. 9. Impedance diagram in the complex plane obtained with a lithium electrode immersed in the molar solution of lithium perchlorate in propylene carbonate. a) after 1 day, b) after 3 days, c) after 4 days.

Fig. 10. Impedance diagram in the complex plane obtained with a lithium electrode immersed in the molar solution of lithium perchlorate in propylene carbonate. a) after 7 days, b) after 8 days, c) after 10 days.

Fig. 11. Impedance diagram in the complex plane obtained with a lithium electrode immersed in the molar solution of lithium perchlorate in propylene carbonate. a) after 11 days, b) after 14 days, c) after 15 days.

Fig. 12. a) Apparent resistance R_a [o] and apparent capacitance C_a [Δ] as a function of the storage time. b) Product R_aC_a as a function of the storage time.

Fig. 13. Thickness of the surface layer as a function of the storage time according to the apparent capacitance for different interphase models. [o] Y, SEI model ($\varepsilon = 5\ \varepsilon_o$). [o] Y, SEI model ($\varepsilon = 10\ \varepsilon_o$). [Δ] L, CSL model ($\varepsilon_1 = 5\ \varepsilon_o$, $\varepsilon_2 = 50\varepsilon_o$). [□] d, CSL model ($\varepsilon_1 = 5\varepsilon_o$, $\varepsilon_2 = 50\varepsilon_o$).

Fig. 14. Thickness of the surface layer as a function of the storage time according to the apparent resistance for different interphase models. [o] Y, SEI model ($\sigma = 1 \times 10^{-9} \Omega^{-1} cm^{-1}$). [•] Y, SEI model, ($\sigma = 2 \times 10^{-9} \Omega^{-1} cm^{-1}$). [Δ] L, CSL model ($\sigma_1 = 1 \times 10^{-9}$, $\sigma_2 = 50 \times 10^{-9} \Omega^{-1} cm^{-1}$). [□] d, CSL model ($\sigma_1 = 1 \times 10^{-9}$, $\sigma_2 = 50 \times 10^{-9} \Omega^{-1} cm^{-1}$).

Fig. 15. Resistances R_i and capacitances C_i as functions of the storage time, according to the SPI model. R_1/C_1, conduction process, R_1/C_1 charge transfer process. R_3/C_3 diffusion process.

Fig. 16. Thickness of the surface layer as a function of the storage time according to the SPI model. [o] for $\sigma = 50 \times 10^{-9} \Omega^{-1} cm^{-1}$. [•] for $\varepsilon = 50 \varepsilon_o$.

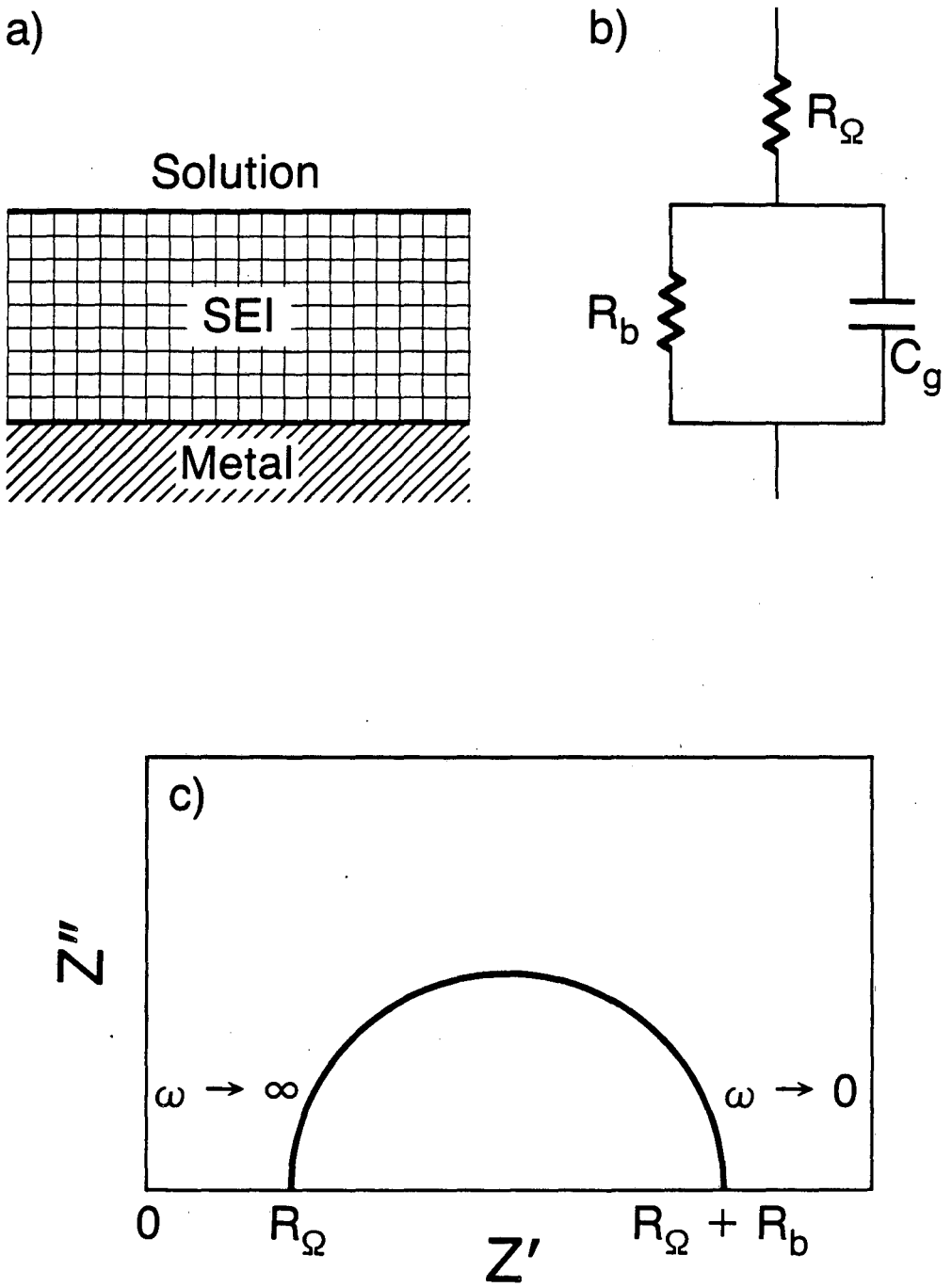

XBL 861-6029

Fig. 1

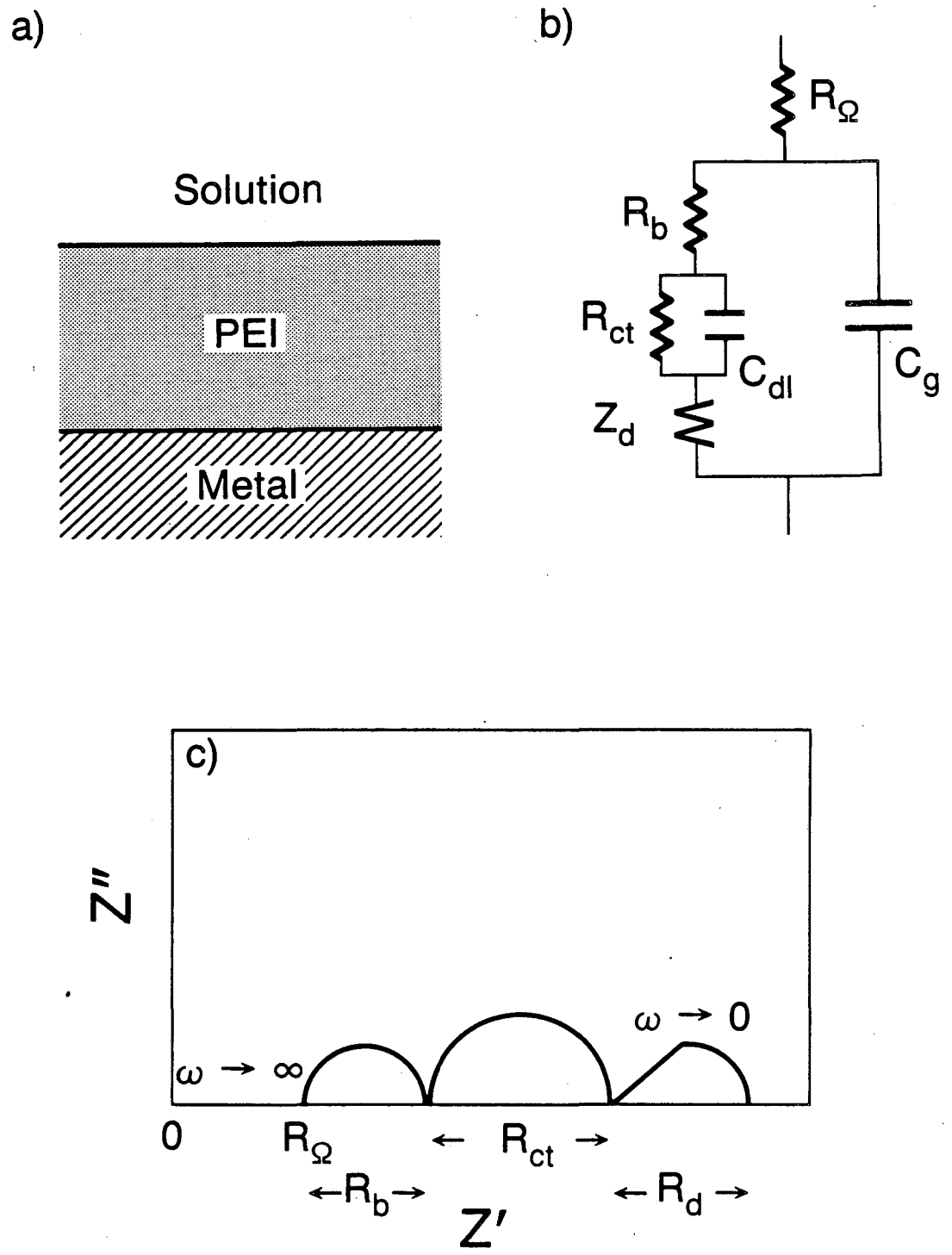

XBL 861-6038

Fig. 2

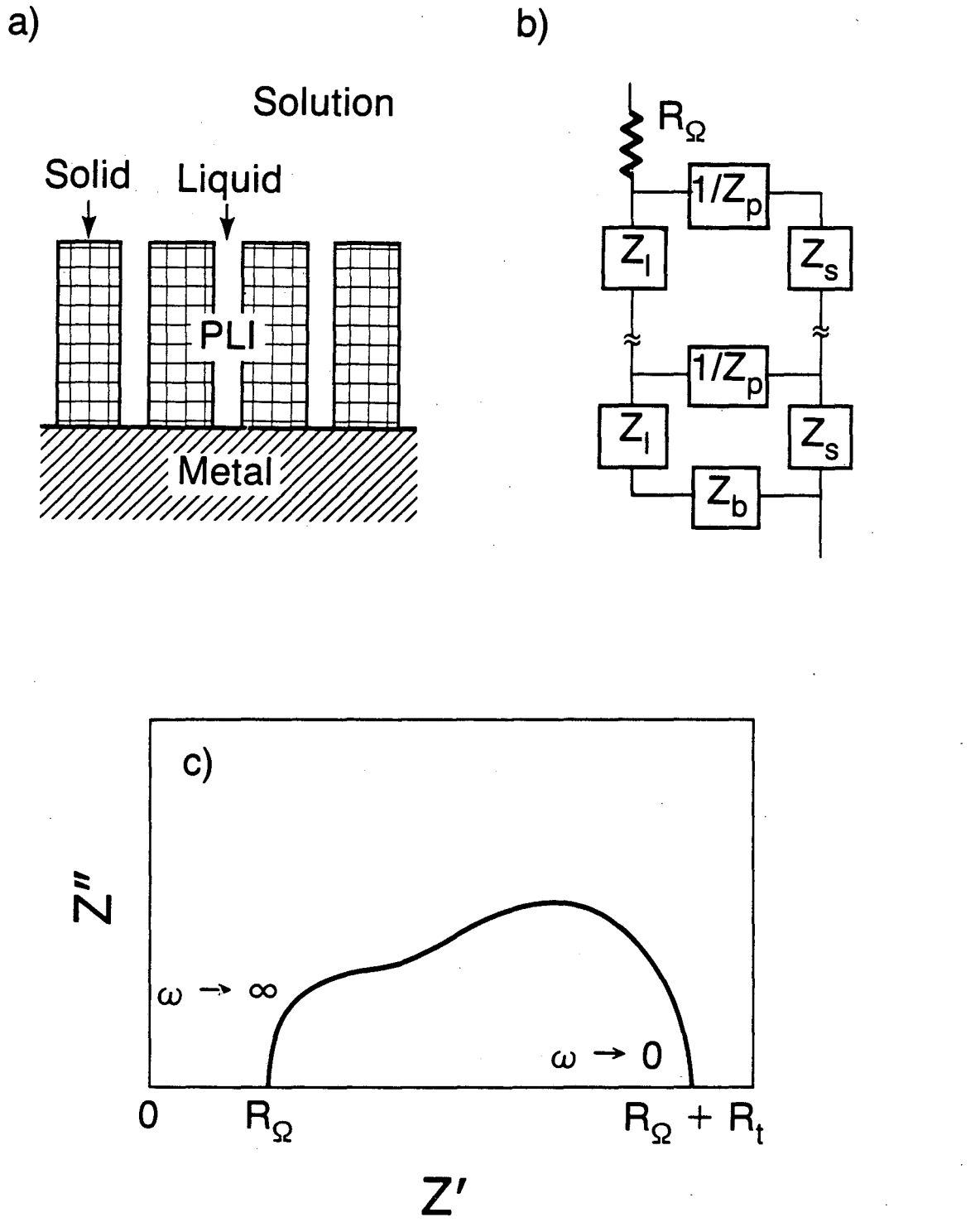

XBL 861-6031

Fig. 3

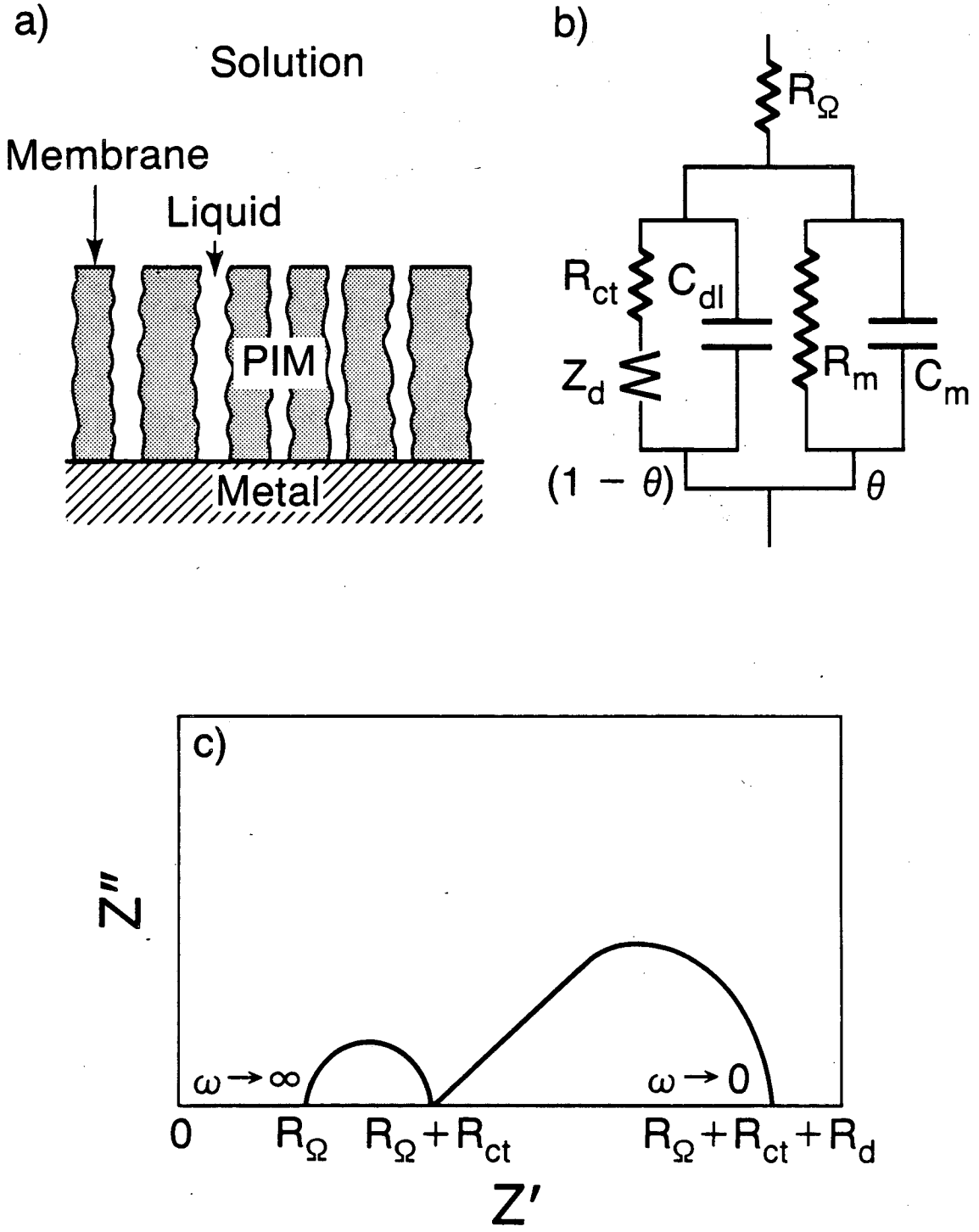

XBL 861-6036

Fig. 4

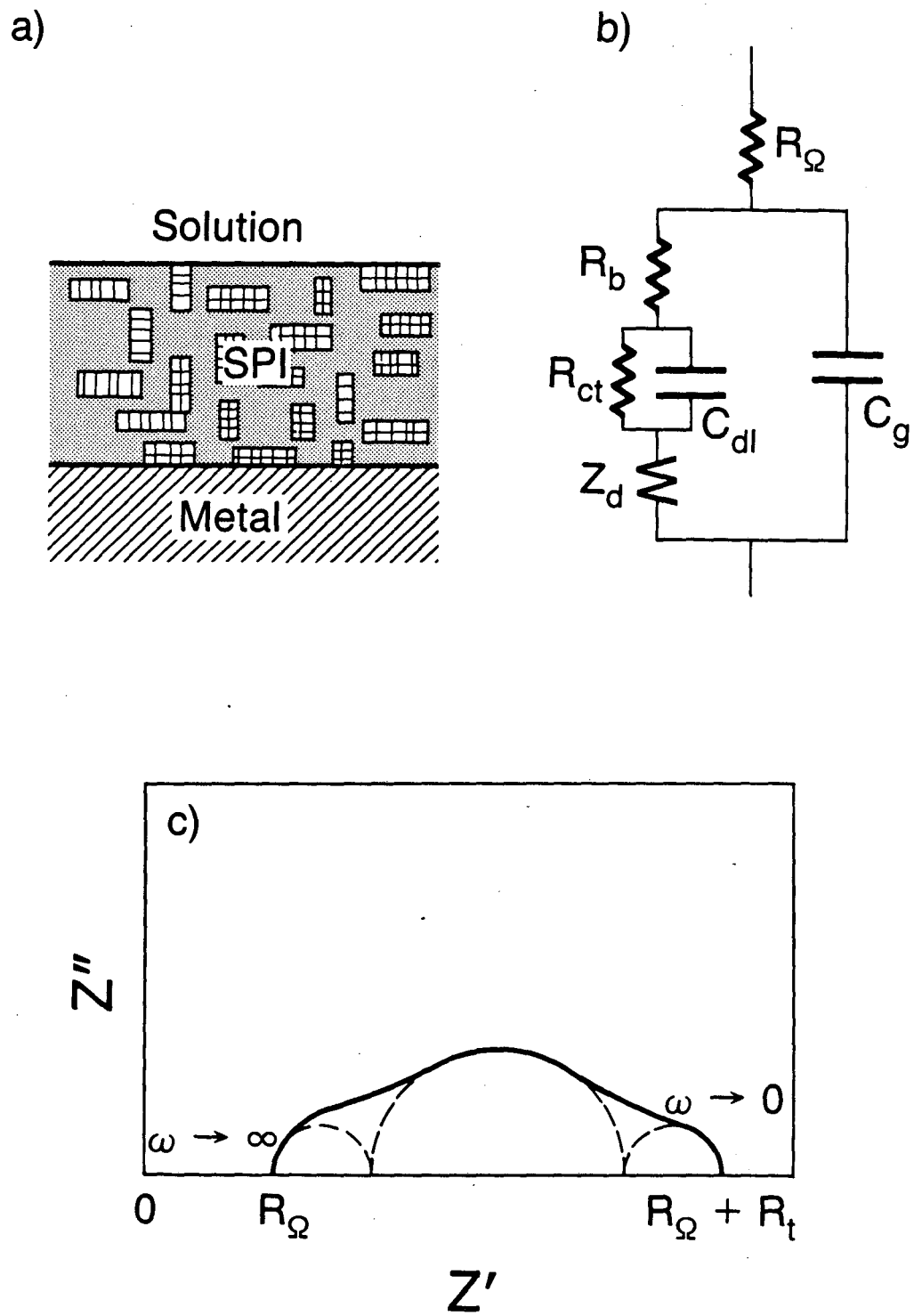

XBL 861-6035

Fig. 5

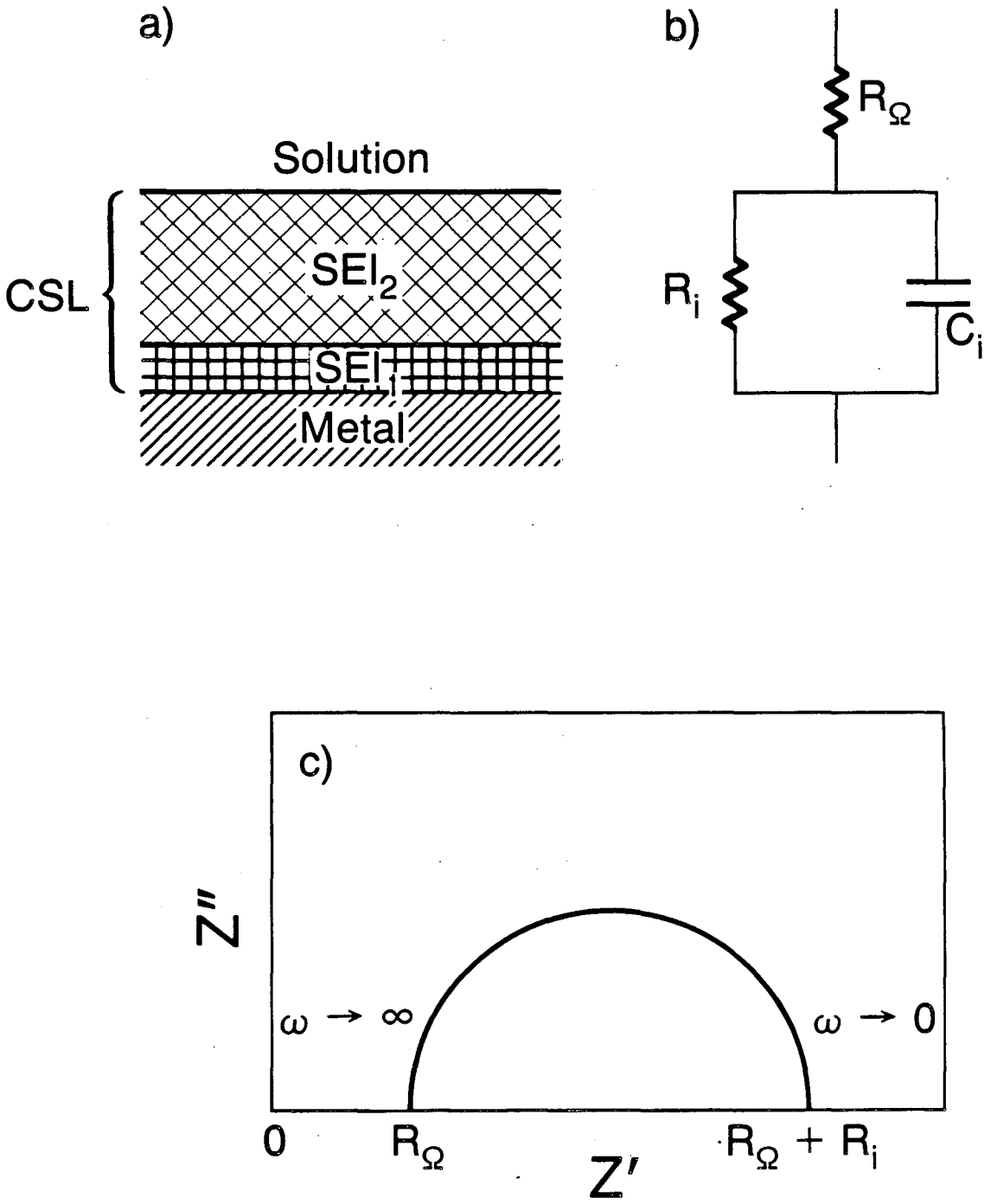

XBL 861-6027

Fig. 6

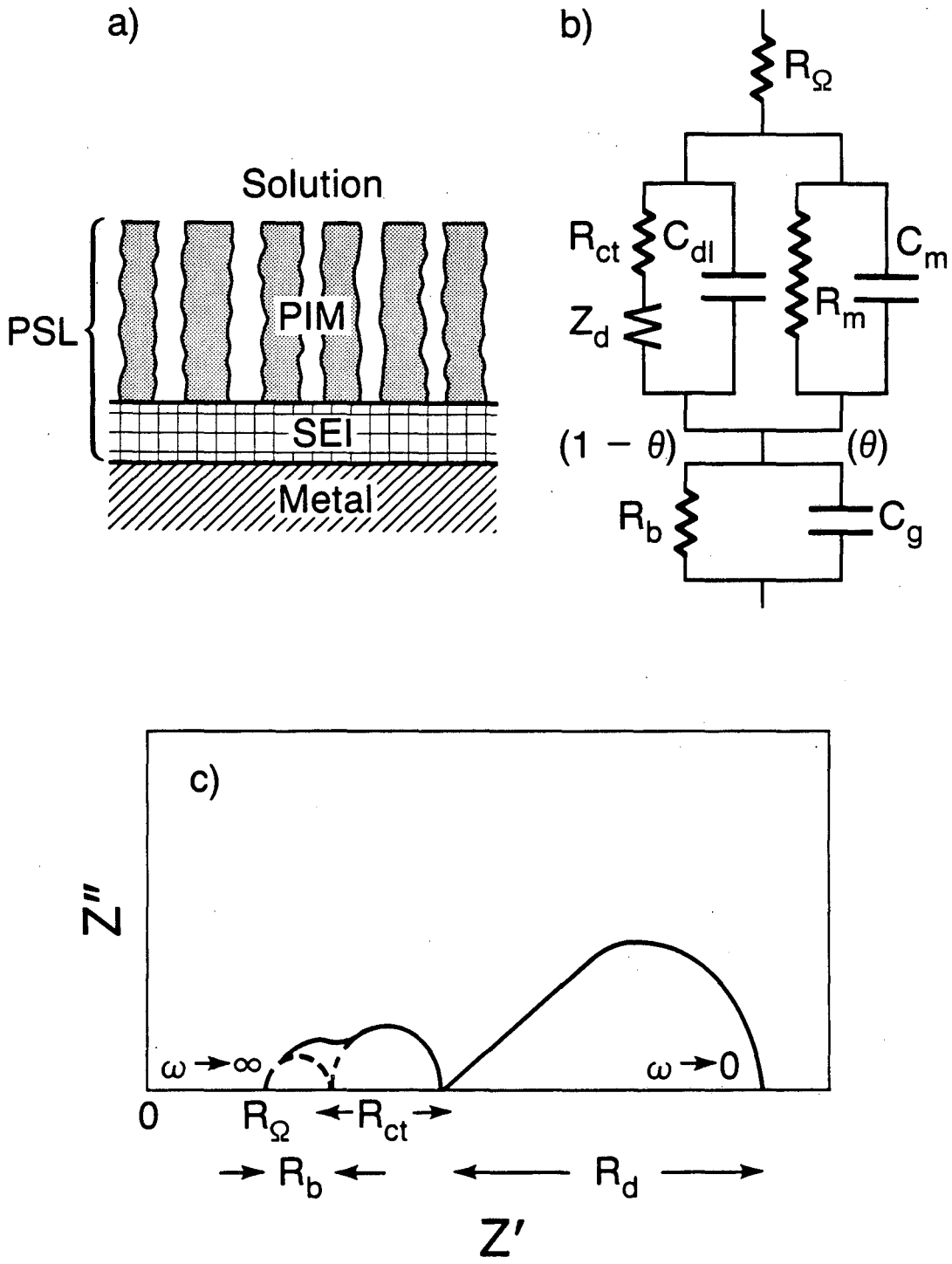

XBL 861-344

Fig. 7

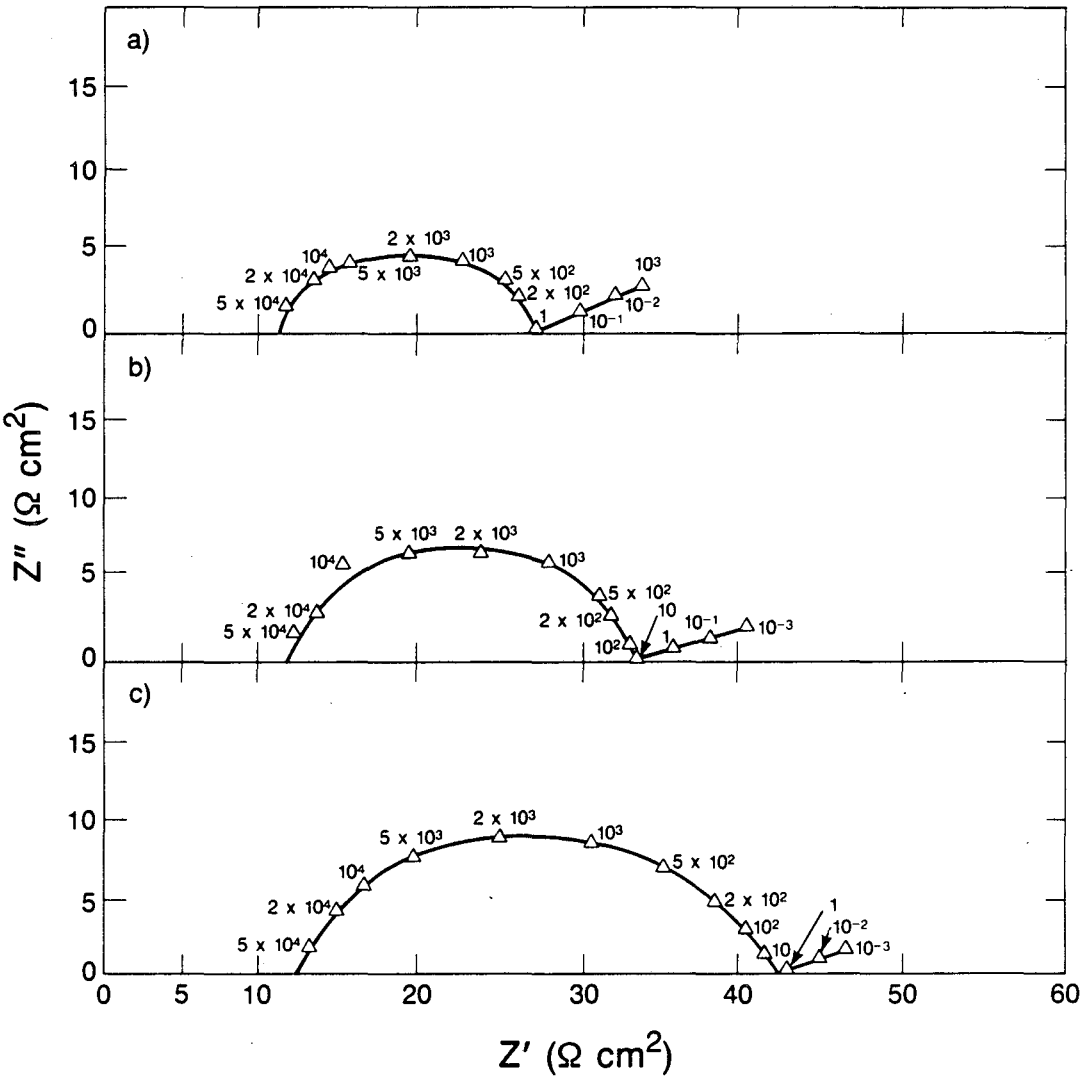
a)
b)
c)
Z'' (Ω cm²)
Z' (Ω cm²)
0
5
10
15
20
30
40
50
60
2 x 10³
10⁴
2 x 10⁴
5 x 10³
10³
5 x 10⁴
5 x 10²
2 x 10²
10²
10⁻¹
10⁻²
10⁻³
1
10
5 x 10³
2 x 10³
XBL 861-6011

Fig. 8

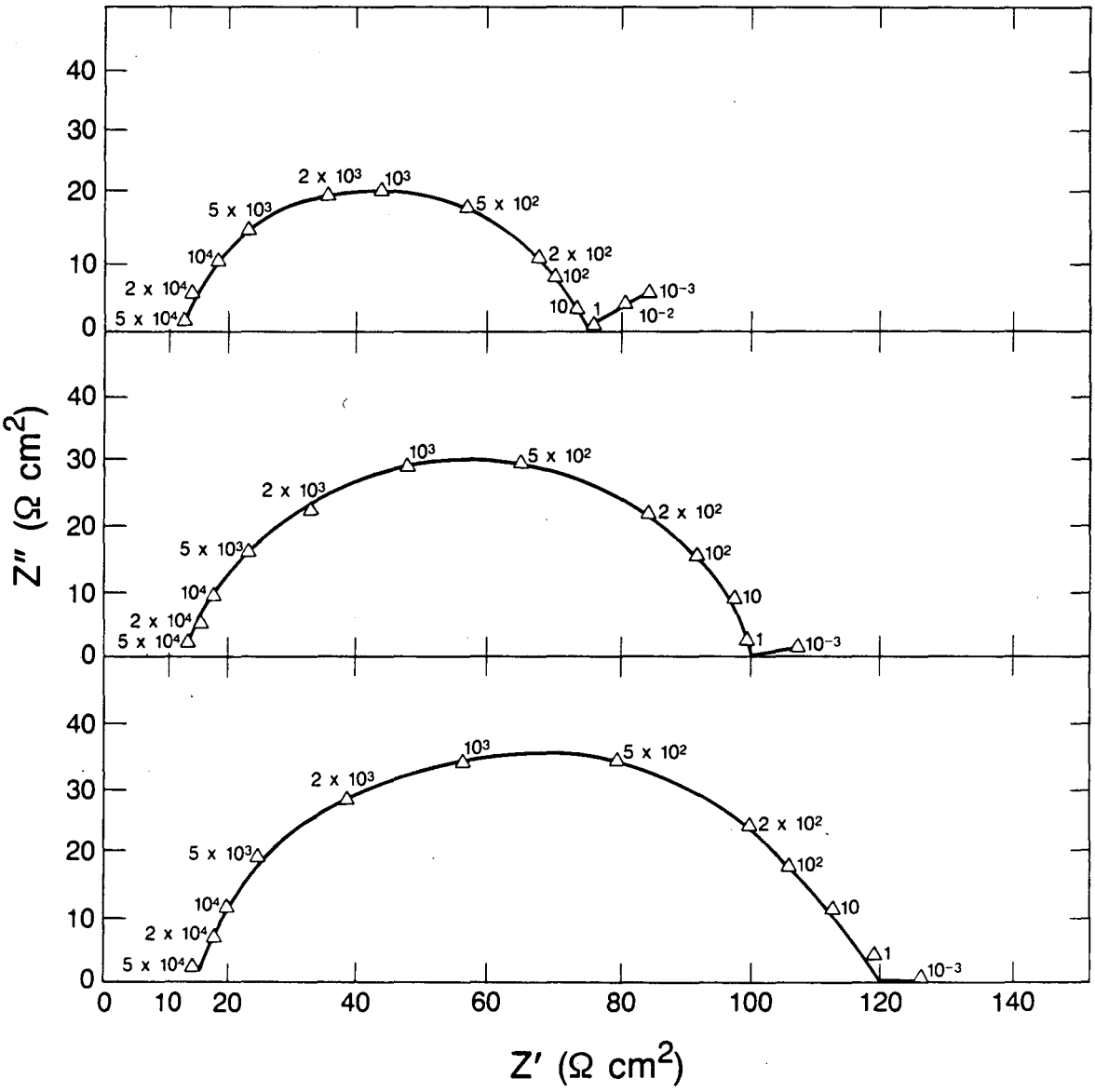

XBL 861-6009

Fig. 9

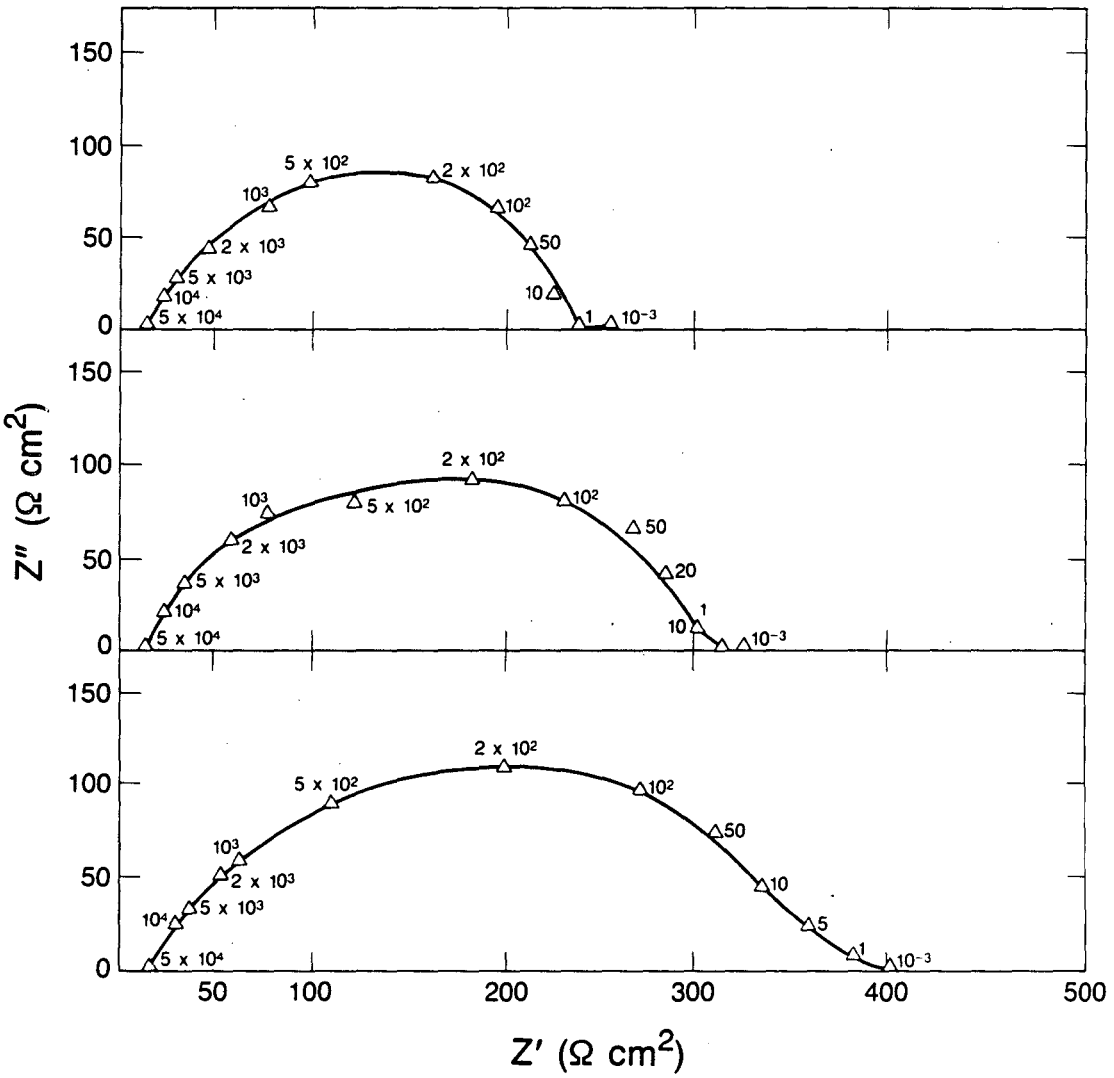
150
100
50
0
Z'' (Ω cm²)
5 x 10²
2 x 10²
10³
10²
2 x 10³
50
5 x 10³
10⁴
10
5 x 10⁴
1
10⁻³
20
5
50
100
200
300
400
500
Z' (Ω cm²)
XBL 861-6010

Fig. 10

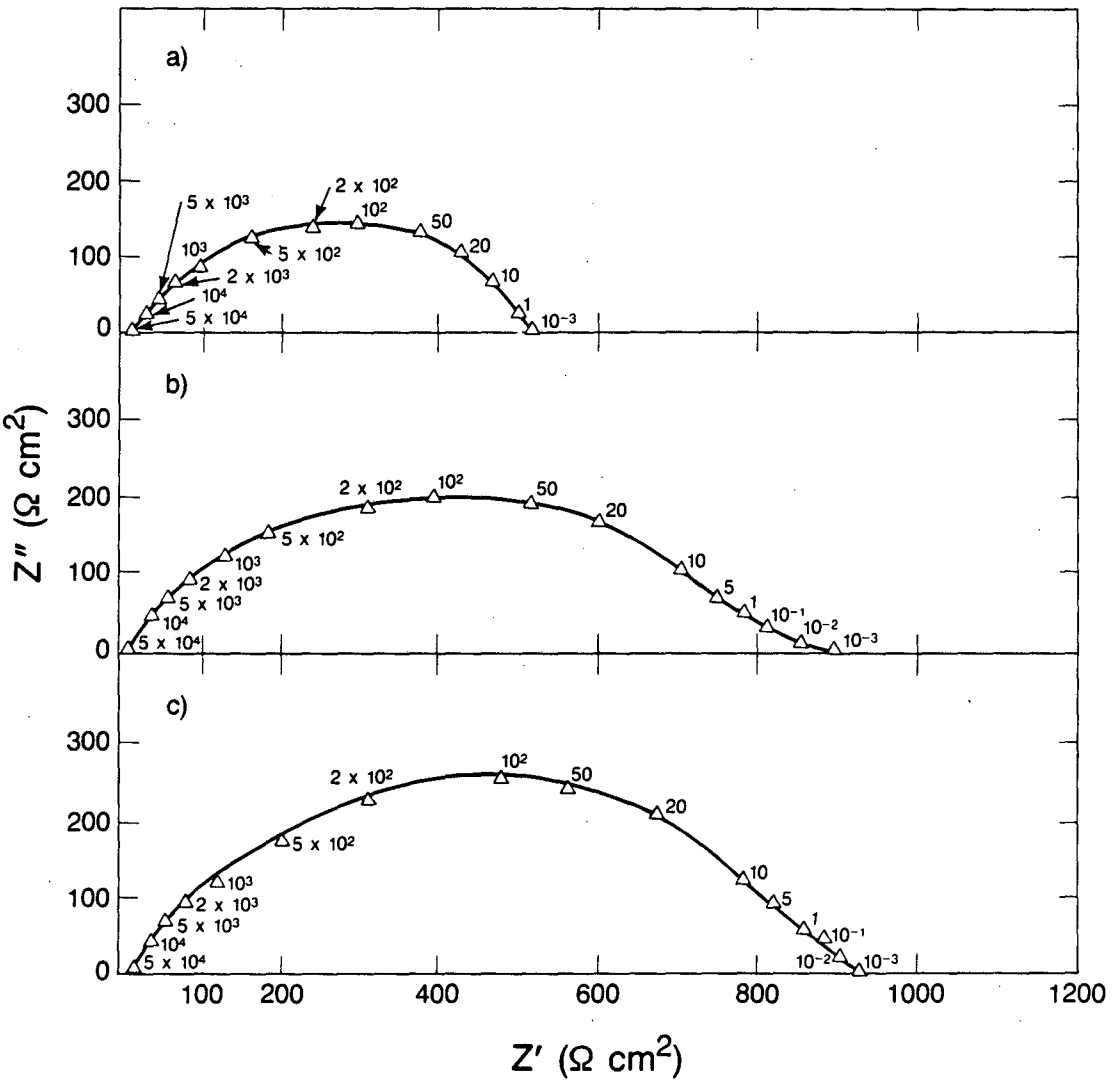

XBL 861-6012

Fig. 11

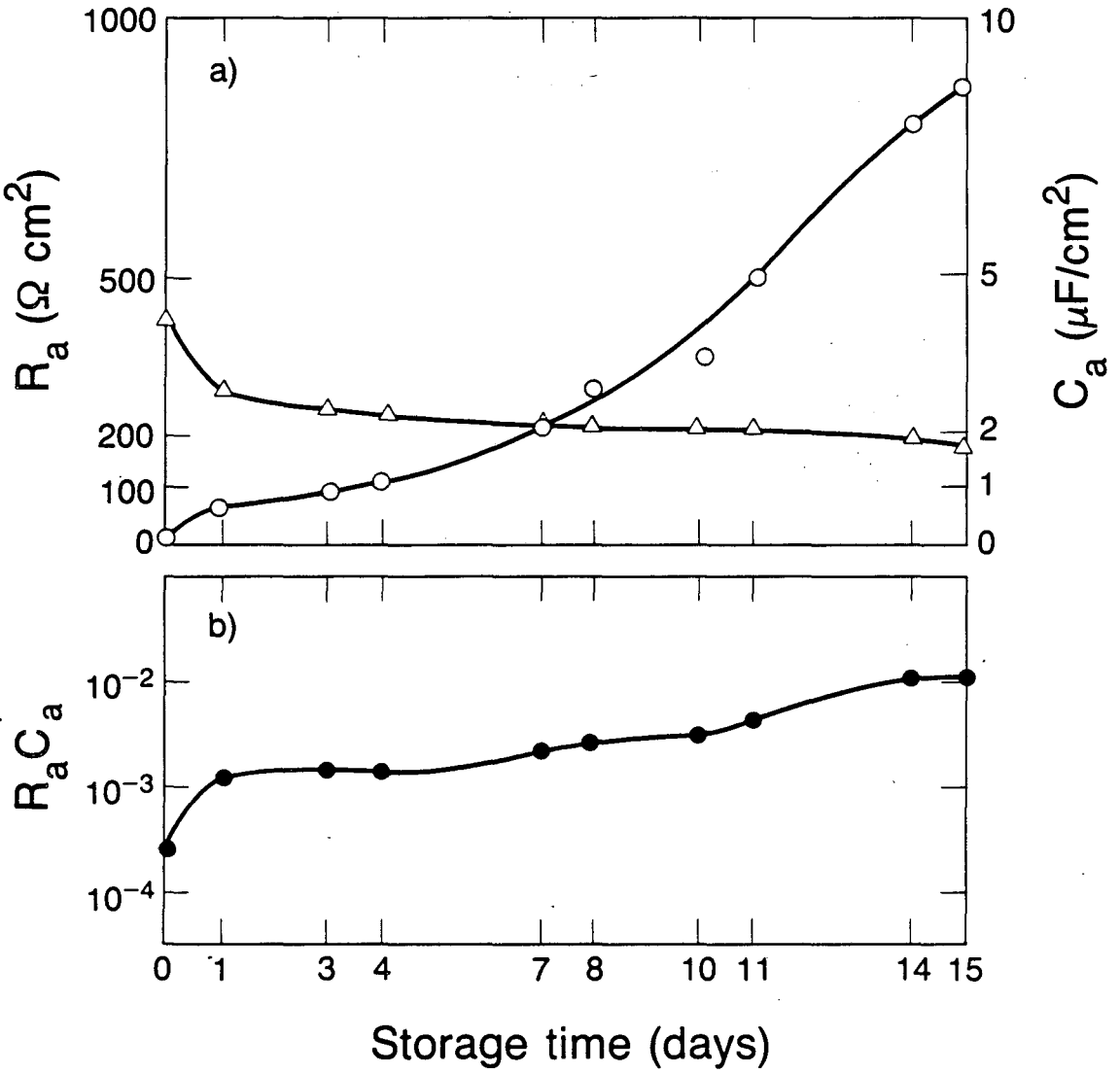

XBL 861-6004

Fig. 12

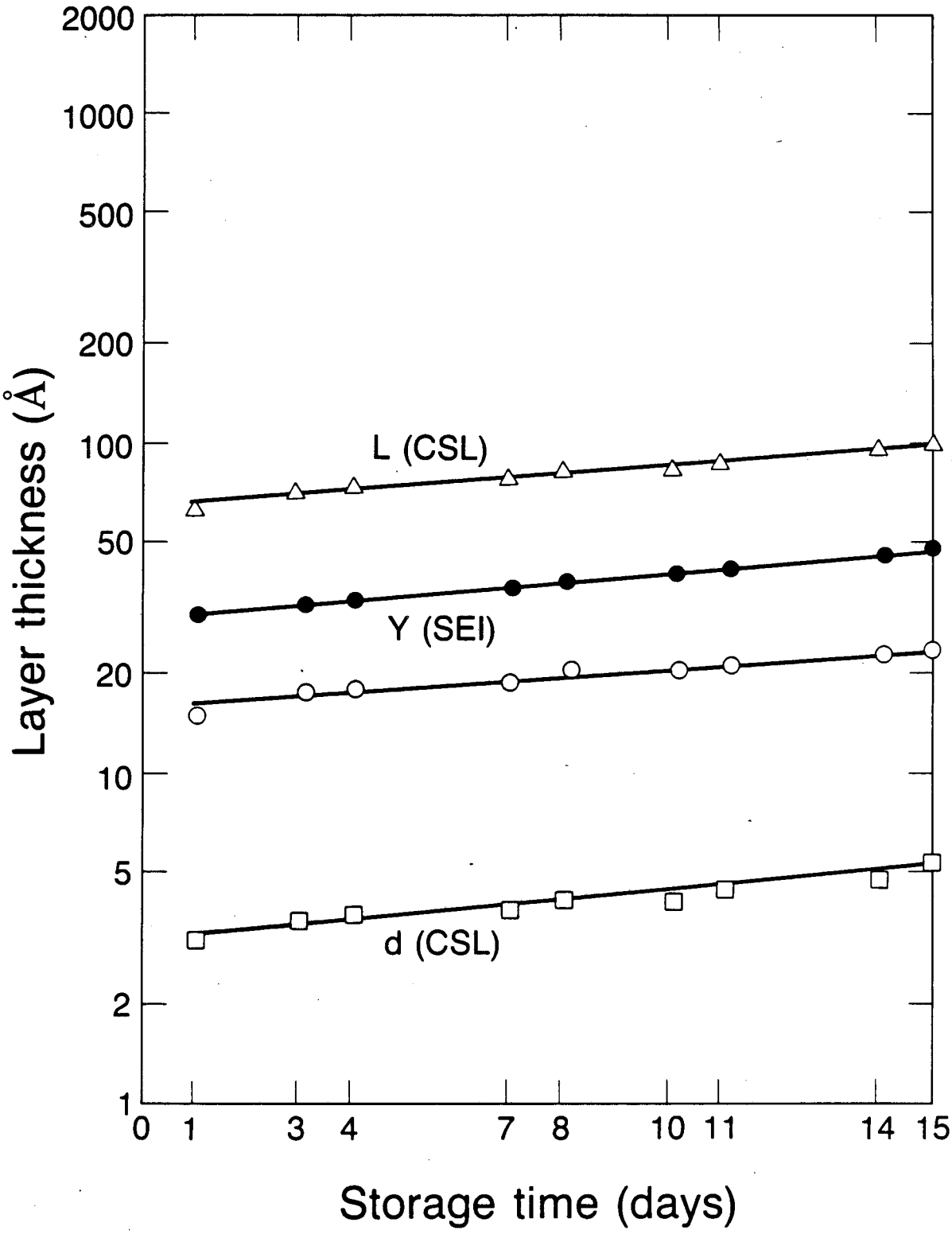

XBL 861-6002

Fig. 13

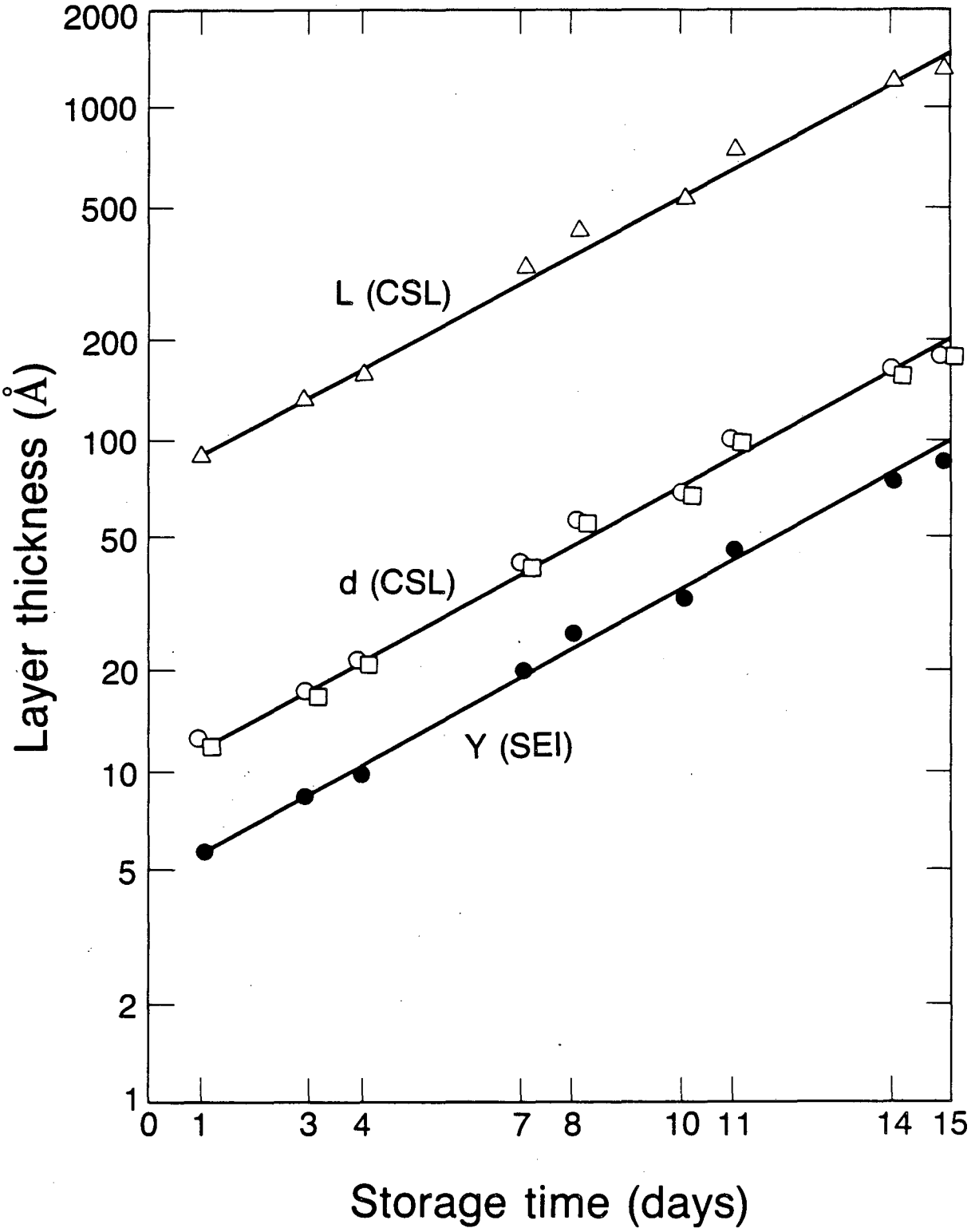
2000
1000
500
200
100
50
20
10
5
2
1
Layer thickness (Å)
L (CSL)
d (CSL)
Y (SEI)
0 1 3 4 7 8 10 11 14 15
Storage time (days)
XBL 861-6001

Fig. 14

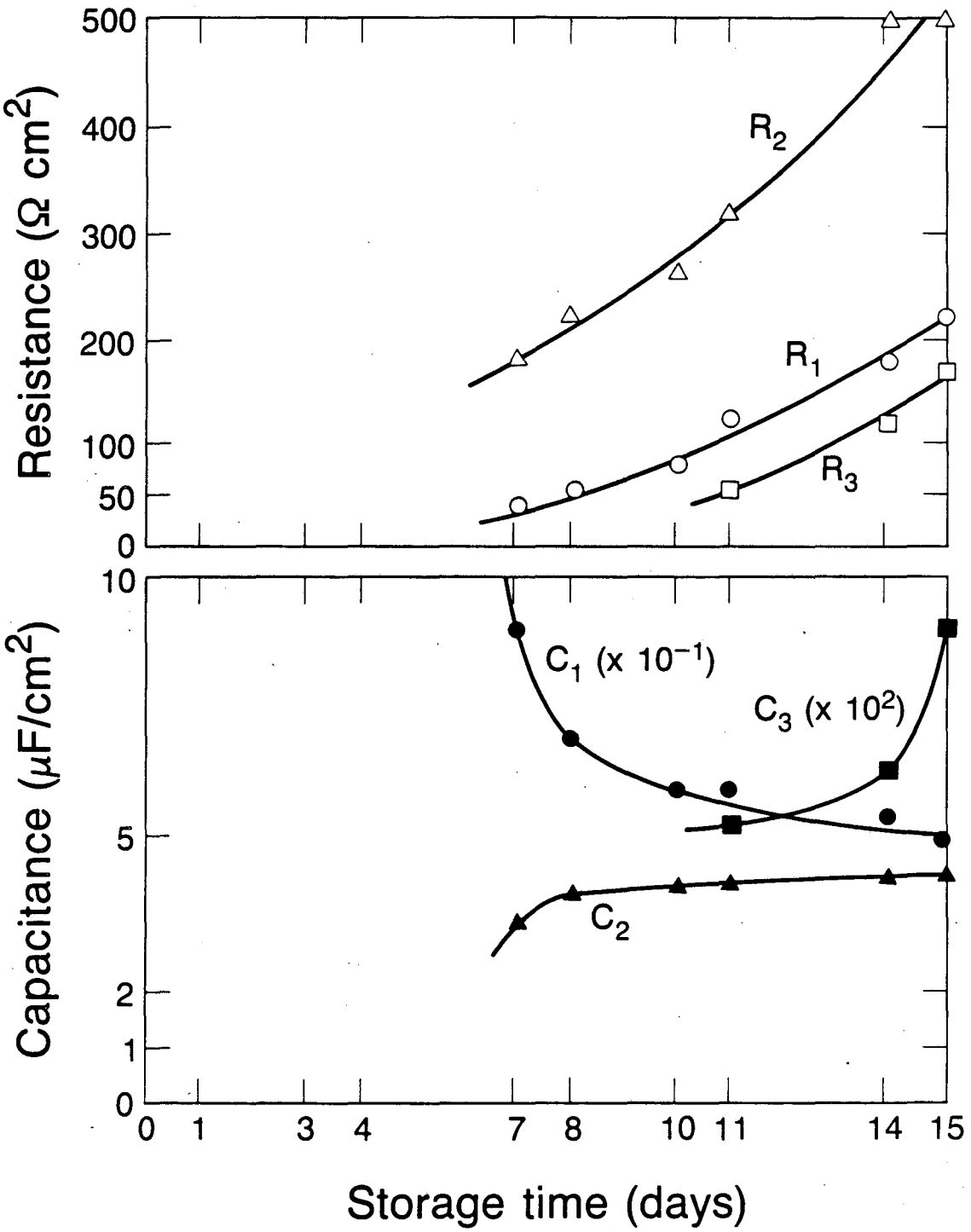
Resistance (Ω cm²)
500
400
300
200
100
50
0
R2
R1
R3
Capacitance (μF/cm²)
10
5
2
1
0
C1 (x 10⁻¹)
C3 (x 10²)
C2
0 1 3 4 7 8 10 11 14 15
Storage time (days)
XBL 861-6003

Fig. 15

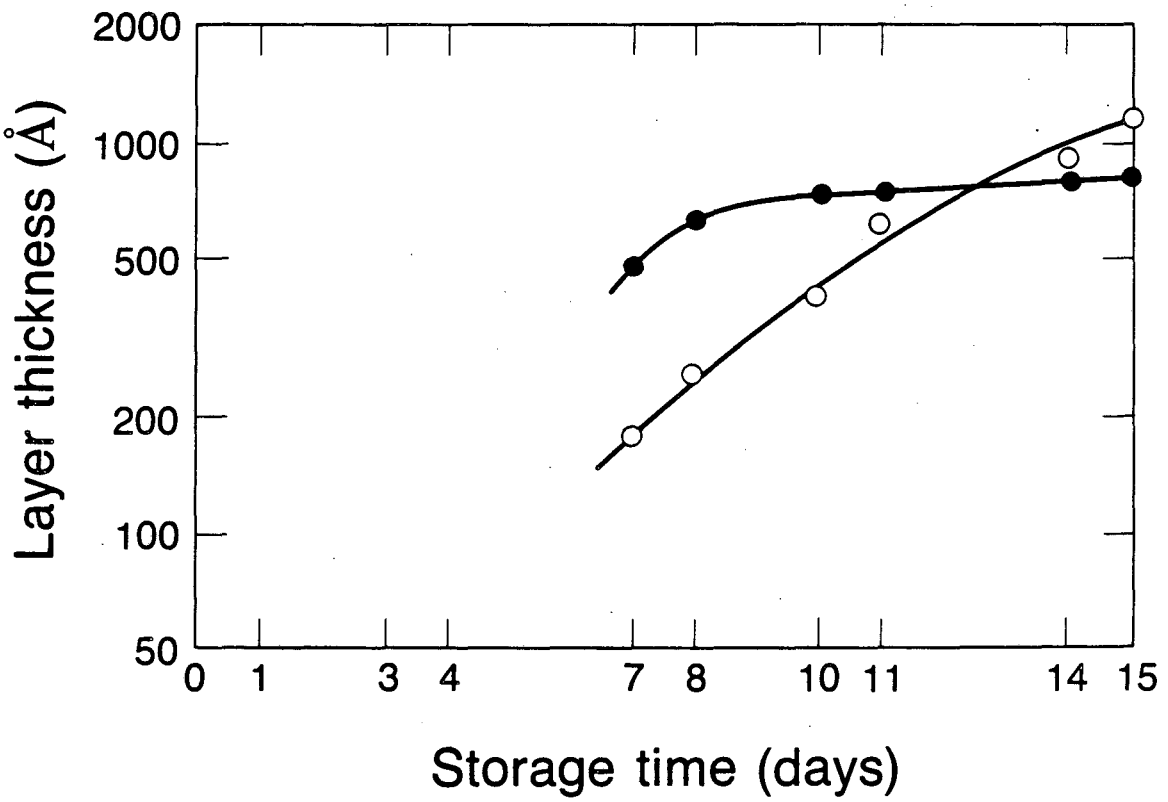
2000
1000
500
200
100
50
Layer thickness (Å)
0
1
3
4
7
8
10
11
14
15
Storage time (days)
XBL 861-6005

Fig. 16

APPENDIX I: Analysis of the SEI and CSL Models

For the case of the Solid-Electrolyte Interphase (SEI) Model, the resistive and dielectric properties of the solid electrolyte are represented by the bulk resistance R_b and the geometrical capacitance C_g. These parameters are related to the conductivity σ and the relative permittivity ε_r in the planar system unit surface area as follows:

$$R_b = Y/\sigma \qquad [1]$$

$$C_g = \varepsilon_r \varepsilon_o / Y \qquad [2]$$

where Y is the thickness of the solid electrolyte, and ε_o is the permittivity of the vacuum.

For the case of the Compact-Stratified Layer (CSL) Model, the surface layer is assumed to consist of two successive sublayers of different limiting permittivities (ε_1, ε_2) and conductivities (σ_1, σ_2). The equivalent circuit of this system consists a priori of two R_b/C_g circuits placed in series. When the time constants of these circuits are not well separated, the impedance diagram in the complex plane exhibits over the whole frequency range only one loop which can be characterized by the apparent resistance R_a and capacitance C_a. Accordingly, a mathematical model of the resistive and dielectric properties of the surface layer can be developed by considering the integral values of the resistance and capacitance for the case where

the permittivity and conductivity are functions of the thickness of the surface layer. For this purpose, as shown in Fig. A1, two main regions can be defined in the surface layer of total thickness L: the thickness d of the first sublayer, and the thickness (L-d) of the second sublayer. In an attempt to understand the properties of this kind of surface layer, an inverse function of second order f(z) has been used for the inverse of the conductivity 1/ (z) and of the permittivity 1/ (z) with the following boundary conditions for f(z):

$$f_2(z) = \frac{f_2}{1+(z/L)^2} \quad \text{for} \quad 0 \leqslant z < (L-d) \qquad [3]$$

$$f_1(z) = f_1 \quad \text{for} \quad (L-d) < z \leqslant L \qquad [4]$$

where z is the distance from the top to the bottom of the surface layer. When d << L, the thicknesses d and L are related to the ratio f_2/f_1 by

$$L/2d \simeq f_2/f_1 \qquad [5]$$

according to the condition $f_2(L-d) = f_1(L-d)$, where f_1 and f_2 are the limiting values of each parameter for the second and first sublayers, respectively.

Thus, the equation of the integral of f(z) for the total thickness L is expressed by:

$$F = \int_{0}^{L-d} f_2(z)\, dz + \int_{L-d}^{L} f_1(z)\, dz \qquad [6]$$

$$F = (f_2 L/2)\, \mathrm{Log}(2L/d) + f_1 d \qquad [7]$$

Taking into account either the conductivity or the permittivity of a thin first sublayer and a thick second sublayer, the integral values of the resistance and capacitance of the surface layer deduced from Eqs. 5 and 7 are given by:

$$R_b = (L/2\sigma_2)\, [1 + \log(4\sigma_2/\sigma_1)] \qquad [8]$$

$$C_g = (2\varepsilon_2/L)\, [1 + \log(4\varepsilon_2/\varepsilon_1)]^{-1} \qquad [9]$$

These Eqs. 8 and 9 deduced from the CSL model can be compared to Eqs. 1 and 2 deduced from the SEI model. Taking the same values of the resistance or capacitance, it is possible to evaluate the ratio L/Y as a function of the ratio f_2/f_1 when considering that the first sublayer of the CSL layer has the properties of a SEI layer:

$$L/Y = \left\{ (f_1/2f_2)[1 + \text{Log } (4f_1/f_2] \right\}^{-1}$$

Under these assumptions, for example for a ratio f_2/f_1 equal to 10 (50), the total thickness L of the CSL layer is 4.25 (15.5) times larger than the thickness Y of the SEI layer. Besides, the thickness d of the first sublayer is nearly 0.05 (0.01) times lower than the total thickness.

APPENDIX II: Analysis of the PEI and SPI Models

For the case of a Polymer-Electrolyte Interphase (PEI) model, the properties of the surface layer can be defined according to the conduction, charge transfer, and diffusion processes. The bulk resistance R_b and the geometric capacitance C_g are related to the conduction process. The charge-transfer resistance R_{ct} and the double-layer capacitance C_{dl} are coupled for the charge-transfer process. The diffusion impedance Z_d for a finite thickness of the diffusion layer is characteristic of the diffusion process.[29] In general, when the time constants of the processes are well separated, the impedance diagram in the complex plane contains three distinct loops over the whole frequency range. The analysis of the conduction semicircle in the high-frequency range leads to the determination of the thickness of the surface layer by using Eqs. 1 and 2 of the resistance and capacitance when either the conductivity or the permittivity of the polymer electrolyte is known.

For the case of the Solid-Polymer Interphase (SPI) model, it is assumed that the properties of the surface layer are essentially those of a polymer electrolyte altered by inclusion of different solid electrolytes. Thus the shape of the impedance diagram can be changed to form only one distorted loop over the whole frequency range. Two main effects are responsible: (1) the dispersion of the time constants for each process; (2) the overlapping of the time constants for successive processes. These effects are detailed below.

Significant distortion in the shape of the impedance diagram occurs when the time constants of successive processes represented by R_i/C_i circuits placed in series are not well separated.[34] For example, the total impedance Z for two circuits can be written as:

$$Z = \sum_{i=1}^{2} \frac{R_i}{1+j\omega R_i C_i} \qquad [11]$$

where $[R_i C_i]^{-1} = \omega_i$ is proportional to the time constant of the R_i/C_i circuit. The corresponding impedance diagram in the complex plane shows two distinct semicircles over the whole frequency range when the ratio ω_1/ω_2 is higher than 100, while only one distorted loop is observed when the same ratio is lower than 10, leading to the overlapping of the time constants. The dispersion of the time constants for a given process represented by a pseudo RC circuit is responsible for a depressed semicircle observed for the impedance plot in the complex plane. The equation of the semicircle, the center of which lies below the real axis, is given by the Cole-Cole formula:[35]

$$Z_\alpha = \frac{R}{1+(j\omega RC)^{(1-\alpha)}} \qquad [12]$$

where α is the depression parameter. It is also related to the angle $\Theta = \alpha\pi/2$ between the radius of the semicircle and the real axis in the complex plane.

The analysis of the impedance data can be obtained graphically by the Cole-Cole and Bode plots. Figure A2 gives an example for the impedance behavior of the surface layer formed after 11 days of storage of the lithium electrode in the propylene carbonate solution. The Cole-Cole plot exhibits over the whole frequency range a distorted loop which can be constituted by three depressed semicircles. The Bode plot (modulus and angle) confirms the occurrence of three time constants related to the frequencies f_1, f_2, and f_3 which can be detected in the impedance data. According to the SPI model, for which the conduction, charge transfer, and diffusion processes are represented by three R_i/C_i circuits placed in series, a satisfactory geometrical fitting of the experimental plots can be obtained by the theoretical plots for a small depression parameter. In principle, all the information about the solid-polymer interphase can be derived by fitting the measured impedance spectrum with the expected impedance spectrum by assuming the parameters of the equivalent circuit. In practice, however, when considering the number of parameters, the curve-fitting technique is not accurate enough and unique. Thus at this time it is only possible to show that the SPI model is reasonable for the study of the surface layer observed.

REFERENCES

1. G.L. Holleck, K.M. Abraham, and S.B. Brummer, in Power Sources for Biomedical Implantable Applications and Ambient Temperature Batteries, edited by B.B. Owens and N. Margalit, The Electrochem. Soc., Inc., 80-4 (1980) 384.
2. J.O. Besenhard and G. Eichinger, J. Electroanal. Chem. 68 (1976) 1.
3. T. Broadhead and F.A. Trumbore, in 10th International Power Sources Symposium, Brighton, England, (1976) p. 232.
4. M. Garreau and J. Thevenin, J. Microscopie et Spectr. Electron. 3 (1978) 27.
5. M. Froment, M. Garreau, J. Thevenin, and D. Warin, J. Microscopie et Spectr. Electron. 4 (1979) 111.
6. Y. Geronov, F. Schwager and R.H. Muller, Electrochemical Society Meeting, Hollywood, FL, 10/5-10/80, Vol. 80-2, Ext. Abs. No. 37, p. 702.
7. J.P. Contour, A. Salesse, M. Froment, M. Garreau, J. Thevenin and D. Warin, J. Microscopie Spectr. Electron. 4 (1979) 483.
8. F. Schwager, Y. Geronov and R.H. Muller, J. Electrochem. Soc. 132 (1985) 285.
9. G. Nazri and R.H. Muller, J. Electrochem. Soc. 132 (1985) 2050.
10. S.G. Meibuhr, J. Electrochem. Soc. 117 (1970) 56.
11. R.F. Scarr, J. Electrochem. Soc. 117 (1970) 295.

12. B. Burrows and S. Kirkland, J. Electrochem. Soc. 115 (1958) 1164.

13. Y. Geronov, F. Schwager and R.H. Muller, J. Electrochem. Soc. 129 (1982) 1422.

14. M. Garreau and J. Thevenin, Electrochemical Society Meeting, Washington, DC, 10/9-14/83, Vol. 82-2, Ext. Abs. No. 308, p. 495.

15. R. Jasinski, in Advances in Electrochemistry and Electrochemical Engineering, edited by P. Delahay and C.W. Tobias, Interscience Publishers, Vol. 8 (1971), p. 253.

16. K.M. Abraham and S.B. Brummer, in Ambient Temperature Lithium Batteries, edited by J.P. Gabano, Academic Press, London, (1983), p. 371.

17. A.N. Dey and B.P. Sullivan, J. Electrochem. Soc. 117 (1970) 222.

18. F.P. Dousek, J. Jansta and L. Riha, J. Electroanal. Chem. 46 (1973) 281.

19. A.N. Dey, Thin Solid Films, 43 (1977) 131.

20. E. Peled, in Ambient Temperature Lithium Batteries, edited by J.P. Gabano, Academic Press, London (1983), p. 43.

21. M. Garreau, J. Thevenin and D. Warin, in Progress in Batteries and Solar Cells, edited by A. Kozawa et al., JEC Press, Inc., Vol. 2 (1979), p. 54.

22. M. Garreau, J. Thevenin, D. Warin and P. Campion, in Lithium Nonaqueous Battery Electrochemistry, edited by E.B. Yeager, et

al., The Electrochemical Society, Inc., 80-7 (1980), 158.

23. G. Nazri and R.H. Muller, 35th Meeting of the International Society of Electrochemistry, Berkeley, CA, (1984) p. 240.

24. G. Nazri and R.H. Muller, J. Electrochem. Soc., 132 (1985) 2054.

25. W.I. Archer and R.D. Armstrong, in Electrochemistry Specialist Periodical Reports, edited by H.R. Thirsk, The Chemical Society, Burlington House, London, Vol. 6 (1980), p. 157.

26. R.D. Armstrong, M.F. Bell and A.A. Metcalfe in Electrochemistry Specialist Periodical Reports, edited by H.R. Thirsk, The Chemical Society, Burlington House, London, Vol. 6 (1978), p. 98.

27. M. Armand, in Workshop on Lithium Nonaqueous Electrochemistry, The Electrochemical Society, Inc., 80-7 (1980) p. 261.

28. M. Armand, Solid State Ionics 9/10 (1983) 745.

29. J.L. Dawson and D.G. John, J. Electroanal. Chem. 110 (1980) 37.

30. J.R. Park and D.D. MacDonald, Corrosion Science 23 (1983), 295.

31. J. Thevenin, C.R. Acad. Sci., Paris, France, 294 (1982) 697.

32. J. Thevenin, J. Power Sources 14 (1985) 45.

33. D.M. Radman, Electrochemical Society Meeting, New Orleans, LA, 10/7-12/84, Vol. 84-2, Ext. Abs. No. 125, p. 188.

34. Y.T. Tasi and D.H. Whitmore, Solid State Ionics 7 (1982), 129.

35. K.S. Cole and R.H. Cole, J. Chem. Phys. 9 (1941), 341.

FIGURE CAPTIONS

Fig. A1. The Compact-Stratified Layer (CSL) Model.

(a) Dependence of the parameter f(z) as a function of the distance z from the top to the bottom of the surface layer. (electrode at z = L).

(b) Ratio L/Y as a function of the ratio f_2/f_1.

Fig. A2. The Solid-Polymer Interphase (SPI) Model.

Analysis of the impedance data obtained after 11 days of storage (cf Fig. 11a).

(a) Cole-Cole Plot

(b) Bode plot (modulus and angle)

The experimental data (Δ) is compared to the theoretical data (o) deduced from an equivalent circuit made of three successive R_i/C_i circuits. R_1 = 120 Ωcm^2, C_1 = 0.6μF/cm^2, R_2 = 320 Ωcm^2, C_2 = 4.1μF/cm^2, R_3 = 60 Ωcm^2, C_3 = 530μF/cm^2. A same depression parameter α= 0.15 has been used for each elementary circuit.

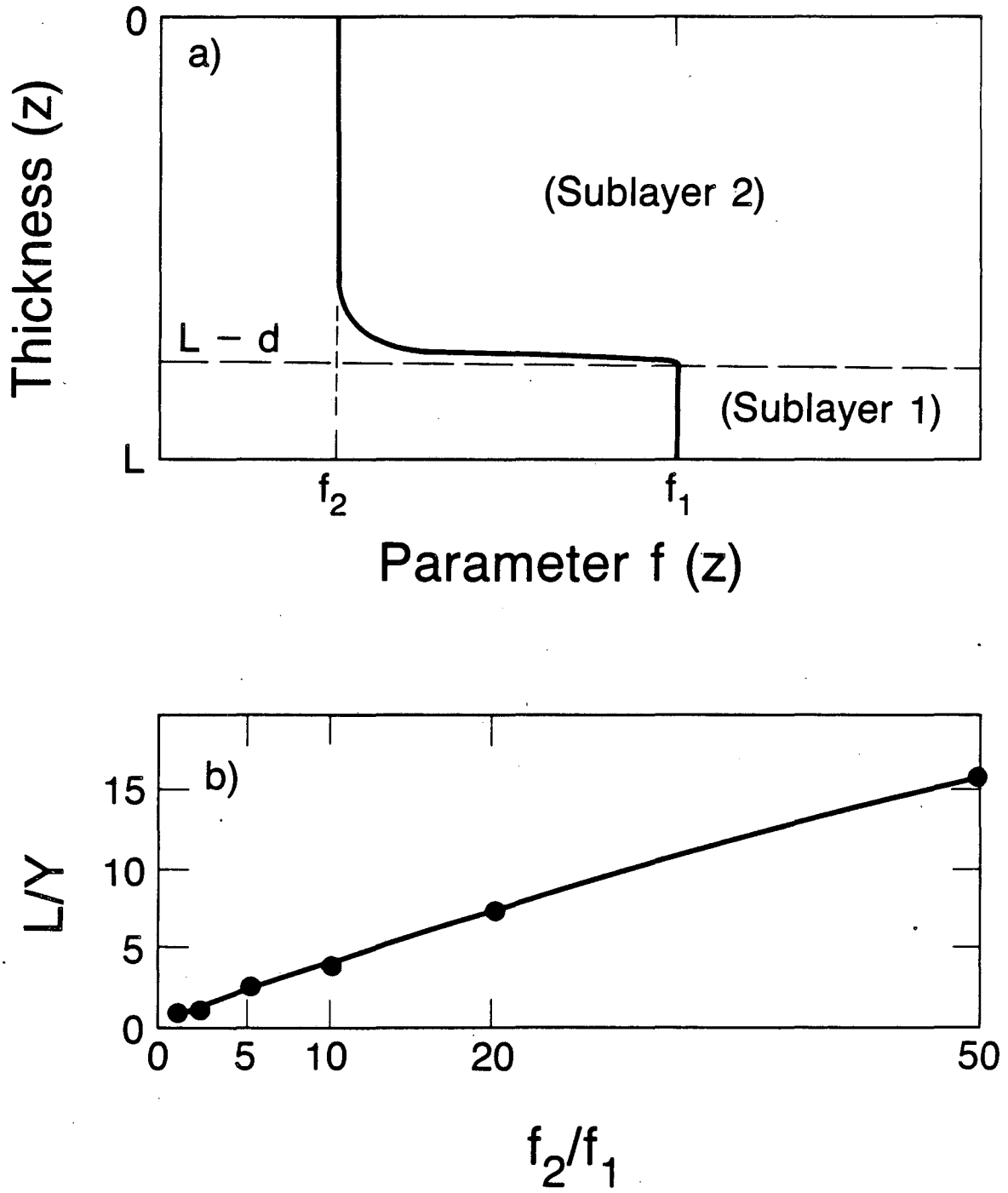

XBL 861-6006

Fig. A1

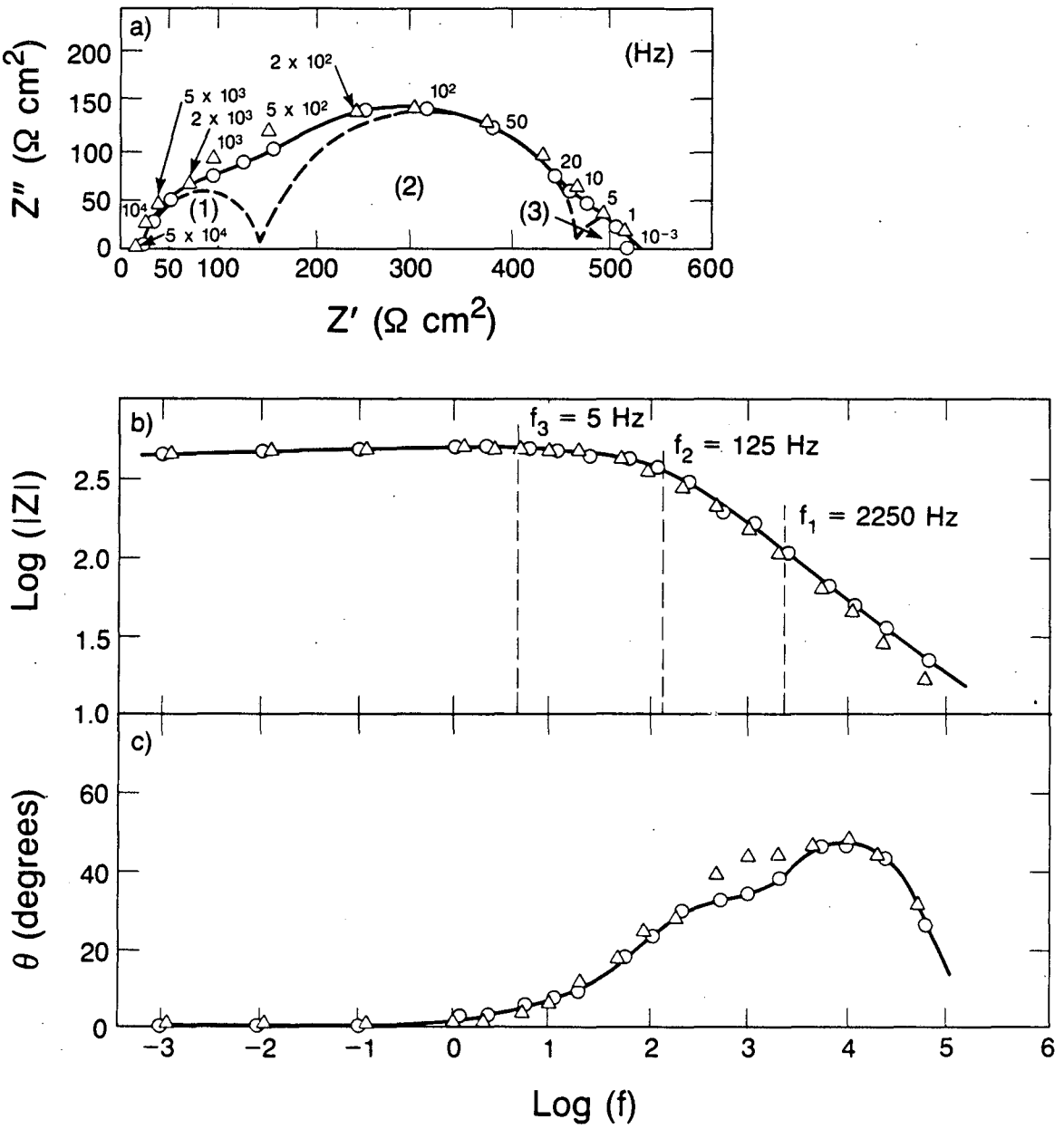
a)
(Hz)
2 x 10²
5 x 10³
2 x 10³
5 x 10²
10³
10²
50
20
10
5
1
10⁻³
10⁴
5 x 10⁴
(1)
(2)
(3)
Z'' (Ω cm²)
Z' (Ω cm²)
b)
f₃ = 5 Hz
f₂ = 125 Hz
f₁ = 2250 Hz
Log (|Z|)
c)
θ (degrees)
Log (f)
XBL 861-6025

Fig. A2

LAWRENCE BERKELEY LABORATORY
TECHNICAL INFORMATION DEPARTMENT
UNIVERSITY OF CALIFORNIA
BERKELEY, CALIFORNIA 94720